Biogeochemistry (2012) 109:151–162
DOI 10.1007/s10533-011-9616-9

Uncoupled surface and below-ground soil respiration in mangroves: implications for estimates of dissolved inorganic carbon export

Daniel M. Alongi · Narciso A. de Carvalho · Aleixo L. Amaral · Akasio da Costa · Lindsay Trott · Frank Tirendi

Received: 3 March 2010 / Accepted: 20 June 2011 / Published online: 15 July 2011

Abstract Potential disparities between rates of surface and below-ground respiration were examined in seven mangrove forests of different topographic height in Timor Leste. Differences in surface respiration between air-exposed and inundated soils were inconsistent, but surface respiration rates increased, with tidal elevation. Net primary production (NPP) on air-exposed soils declined with increasing forest cover indicating light limitation beneath the canopy. NPP and respiration were linearly related under both air-exposed and inundated conditions. Rates of DIC release from the soil surface varied among forests, correlating only with soil carbon (TOC) and nitrogen (TN) and their stoichiometric ratios. Sulfate reduction was detected to maximum depth of unconsolidated soil, correlating only with TOC and TN content at discrete depth intervals. DIC concentrations in drainage channels were equivalent to porewater concentrations. The rate of carbon mineralized by sulfate reducers (SRC) was equivalent to rates of total carbon oxidation (TCO) measured at the soil surface in forests at tidal heights $\leq$0.5 m above mean sea-level (MSL). However, SRC was increasingly greater than TCO in forests residing from 1.0 up to 2.5 m above MSL. Most carbon mineralized in subsurface deposits appears to seep out of the forest via groundwater. Rates of surface respiration therefore underestimate rates of total benthic carbon mineralization in forests at topographic heights $\geq$0.5 m above MSL, suggesting that the amount of respiratory carbon exported from many mangrove forests has also been underestimated.

Keywords Carbon · Export · Mangrove · Metabolism · Soil respiration · Timor Leste

Abbreviations

NPP	Net primary production
DIC	Dissolved inorganic carbon
TOC	Total organic carbon
TN	Total nitrogen
SRC	Carbon oxidation via sulfate reduction
TCO	Total carbon oxidation
MSL	Mean sea-level
DBH	Diameter-at-breast height
ABG	Above-ground biomass
LAI	Leaf area index
TP	Total phosphorus
AVS	Acid-volatile sulphide
CRS	Chromium-reducible sulphur
SRR	Sulfate reduction
OW	Overlying tidal water
PW	Porewater

D. M. Alongi (✉) · L. Trott · F. Tirendi
Australian Institute of Marine Science, PMB 3,
Townsville MC, QLD 4810, Australia
e-mail: d.alongi@aims.gov.au

N. A. de Carvalho · A. L. Amaral · A. da Costa
Departamento de Geslav de Recursos Pesqueiros,
Ministeris de Agricultura, Florestas e Pescas, Comoro,
Dili, Timor-Leste

DRO Dark oxygen consumption
DRC Dissolved inorganic carbon release

Introduction

Mangrove forests are among the most productive marine ecosystems, contributing carbon to the coastal ocean disproportionate to their small global area. Rates of mangrove primary production often rival those of tropical rainforests (Alongi 2009). Mangroves are important transition zones between land and tropical seas, having some elements of terrestrial and marine ecosystems. Mangroves are natural buffers against coastal erosion and catastrophic events, such as tsunamis, and are accumulation sites for soil, carbon, contaminants, and nutrients (Saenger 2002).

High rates of net forest primary production are driven partly by tight links between trees, soils, and microbes (Alongi 2005; Lovelock 2008). Processes occurring on and within the forest floor are crucial for how mangroves function and contribute energetically to the coastal ocean. Because of efficient particle trapping, the forest floor serves as a vital reservoir for the accumulation and subsequent decomposition and recycling of organic matter, receiving and storing materials derived from land and sea (Bouillon et al. 2008a, b). The forest floor is usually dominated by crab burrows and deep tree roots, and often pockmarked with cracks and fissures. Coupled with drainage and recharge of the interstitial water by tides and precipitation, these structures and benthic faunal activities foster temporally and spatially complex patterns of organic matter decomposition within the forest floor (Kristensen 2007). Beneath a thin veneer of oxidized soil on the surface, suboxic and anoxic processes dominate early diagenesis in mangrove soils (Kristensen 2007). Sulfate reduction is usually the major anaerobic pathway, occurring to a soil depth of at least 1 m or more, and is most likely related to root uptake and exudation of dissolved materials (Nedwell et al. 1994; Alongi 2005). Complicating the spatial patterns of anoxia is the presence of fine and coarse roots through which some mangrove species translocate oxygen. Grapsid and sesarmid crabs also play a key role in modifying soil properties, exerting some control over benthic microalgal production and pathways of soil metabolism (Kristensen and Alongi 2006; Kristensen 2008).

Factors regulating surface and below-ground microbial processes thus include crab and root activities, grazing, the quantity and quality of organic matter, and water content (Kristensen 2007; Kristensen et al. 2008). However, many of these factors are in turn inextricably linked to environmental factors, especially climate and topography. The ebb and flood of tides greatly influence processes occurring on and within the forest floor; soils less frequently inundated and more air-exposed usually hold less interstitial water or often experience dryness to considerable depths (Alongi et al. 2000) or to the opposite extreme, experience dilution from monsoonal rains (Alongi et al. 2001). At higher tidal levels closer to land, a greater volume of the forest floor experiences tidal oscillations and faster lateral transport of drainage than flood waters, due to factors such as tidal asymmetry, number and complexity of burrows and other openings, soil texture, the extent of groundwater (if any), and slope of the forest floor (Ridd 1996; Heron and Ridd 2008). This subsurface flow is complex (Mazda and Ikeda 2006), but how it affects microbial metabolism within the forest floor is unknown.

Most published studies on forest floor metabolism have focused on measurements of total benthic metabolism that integrate rates of metabolism throughout the entire soil column, or on specific processes, such as sulfate reduction (Alongi 2005, 2009). Much less is known about the conditions under which these integrative and specific measurements relate to one another; for example, the extent to which the decomposition of organic matter is in steady-state or whether or not disequilibrium is induced by environmental cues, such as lateral transport of interstitial water. The few mangrove studies have found discrepancies between rates of subsurface anaerobic metabolism and surface measurements of CO_2 and O_2 flux (Kristensen et al. 1988, 2008; Nedwell et al. 1994; Alongi 2001). Understanding such differences would help to more accurately estimate the amount of respiratory carbon exported to the adjacent coastal ocean (Bouillon et al. 2008a; Alongi 2009).

The main purpose of this study was to test the hypothesis that differences between surface and below-ground rates of benthic metabolism increase with increasing topographic height of mangrove forests, with surface measurements clearly underestimating total soil respiration. Surface and below-ground soil metabolism were therefore measured in mangroves residing across a spectrum of topographic heights along the northern and southern coasts of Timor Leste (East Timor). These measurements were also related to other forest and edaphic characteristics to determine if what other factors regulate surface and below-ground soil respiration.

Study sites and methods

Site description

Seven mangrove forests on the north and south coasts of Timor Leste were chosen to represent low- to high-intertidal mangrove forests common along the Timorese coast (Fig. 1). This region is in the dry tropics with an average annual rainfall of ≤800 mm and a distinct dry season between July and October (Durand 2002). Station TL4 (9°10″S, 125°43″E) was a mid-intertidal stand co-dominated by short (3–4 m height) *Exocoecaria agallocha* and *Lumnitzera racemosa* in compacted fine sand. Station TL5 was located ca. 50 m seaward of Sta. TL4 in the low-intertidal and was co-dominated by taller (10–12 m height) *Rhizophora apiculata* and *Rhizophora stylosa* in fine silt and clay. Both stations were located within a lagoon behind a sandy barrier. Stations BC1, SL1 and SL2 were located in lagoons further west on the south coast (Fig. 1). Station BC1 (9°15″S, 125°24″E) was a mid-intertidal forest dominated by tall (12–15 m height) *Rhizophora mucronata* in fine silt and clay and was located near the landward edge of a sandy lagoon fronted by high sand dunes. Stations SL1 and SL2 (9°21″S, 125°16″E) were located within the same lagoon (Fig. 1) with Sta. SL1 located in the high-intertidal zone and composed of short (4–6 m height) *Sonneratia urama* in fine sand and silt carpeted with microalgal mats. Station SL2 was located in the mid-intertidal ca. 200 m seaward of Sta. SL1 and was dominated by short (3–6 m height) *R. stylosa* interspersed with short *Avicenna marina* and *E. agallocha* in fine sand and silt. On the north coast, station TL6 (8°32″S, 125°42″E) was a low-intertidal forest dominated by tall (20–25 m height) *R. mucronata* interspersed with shorter (10–15 m) *R. stylosa* and tall (45–50 m) *Sonneratia alba* in fine silt and clay. Station TB1 (8°34″S, 125°28″E) was a tall (18–22 m height) *S. alba* stand located in a sheltered sandy embayment. Stations TL4 and TL5 were sampled at the end of the wet season (June 2007) and at the end of the dry season (October 2008). The other stations were sampled once in October 2008.

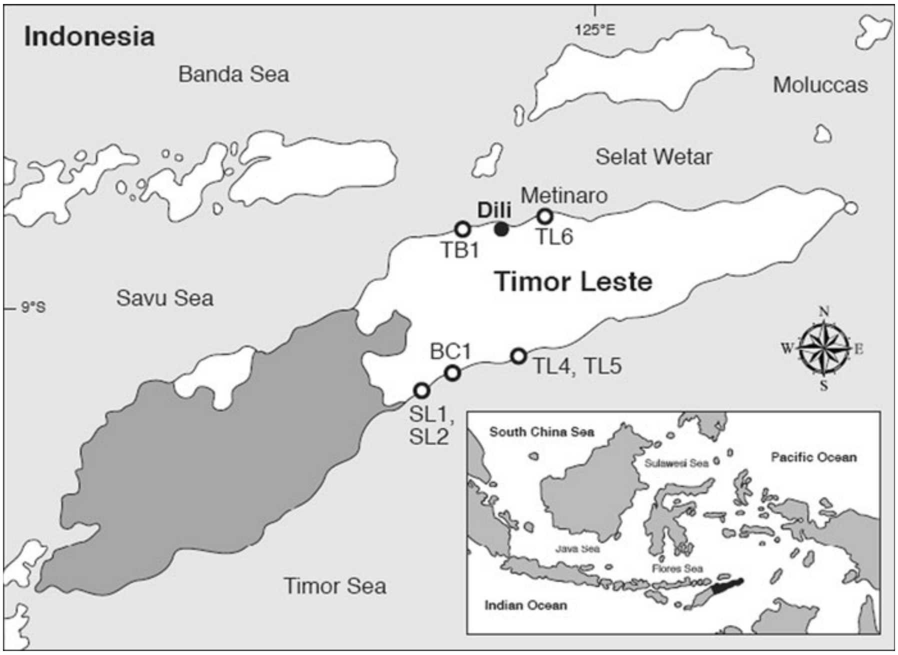

Fig. 1 Map of the seven sampling locations along the northern and southern coasts of Timor Leste. *Insert* map shows the location of Timor Leste in the Australasian region

Forest sampling

Three plots per forest were established using the angle cruising method (Cintron and Novelli 1984; Clough 1997). Briefly, three separate sets of angular sighting measurements were made using a relascope within each forest. The method does not encompass a consistently sized plot but covers an area in accordance with the size class of the trees which fall within the scale used. In these forests, the trees were identified, measured for diameter-at-breast height (dbh) and taped; the center of each semicircular plot was staked for further sampling for soil characteristics and microbial processes (see below). Forest data were used to calculate basal area and stem density which in turn was used to estimate above-ground biomass (AGB) using the allometric relationships in Komiyama et al. (2005) and wood density for these species in Saenger (2002).

Measurements of light absorption by the forest canopy (100–250 light readings per plot taken randomly on sunny days between 1000 and 1400 h) were used to estimate canopy cover ($\eta =$ number of readings under closed canopy divided by total number of readings) and leaf area index (LAI) using the formula:

$$\mathrm{LAI} = \frac{\left[\log_e(\mathrm{I})_{\mathrm{mean}}\right] - \left[\log_e(\mathrm{I_o})_{\mathrm{mean}}\right]}{-\mathrm{k}}$$

where $(\mathrm{I})_{\mathrm{mean}}$ mean PAR under the canopy, $(\mathrm{I_o})_{\mathrm{mean}}$ incident PAR, and k canopy light extinction coefficient (0.5). LAI was corrected for solar zenith angle.

Topographic height was estimated at each site by difference between the predicted height of the high tide for the day (estimated from tide tables) on which measurements were taken and ground level (Clough 1997). These values were checked using a hand-held GPS to measure altitude. Accuracy of this method is ca. 7 cm.

Soil sampling and chemical analyses

During each field sampling, triplicate wells to a depth of ca. 50 cm were made in each plot using a 1.5 m length stainless steel corer (7 cm inner diameter). After waiting 10–15 min for water seepage, triplicate samples were taken for measurement of salinity and DIC. Samples for DIC were also taken at high tide and in obvious drainage channels adjacent to the forests at low tide. The samples were filtered (0.45 µm Minisart® filters), acidified, and kept cool and dark until analysis. DIC concentrations were determined using the procedures of Hall and Aller (1992) and Lustwerk and Burdige (1995). Salinity was determined using a hand-held refractometer. In dry soils at Sta. TL4, soils were wetted just enough with distilled water to obtain a salinity reading and corrected based on later measurement of porewater content.

Soils ($n = 5$) were taken from the cores used to make the wells by extruding the entire core and slicing at 2 cm intervals to maximum core depth. Samples were frozen and on return to the laboratory, dried, and ground to a fine powder for determination of total organic carbon (TOC) on a Shimadzu TOC Analyzer with solid sampler and total nitrogen (TN) on a Perkin-Elmer 2400 CHNS/O Series II Analyzer. Total phosphorus (TP) was determined after strong acid digestion on a Varian Liberty spectrometer following the procedure of Loring and Rantala (1992).

Sulfate reduction

Rates of sulfate reduction were measured from 2.7 cm diameter plastic cores inserted within the 1.5 m length steel corer during insertion into the soil to bedrock or highly compacted soil. Triplicate cores were taken from each plot during exposure and inundation, except at Stas. SL1 and SL2 where triplicate cores were taken only when the surface was exposed. Samples were also taken within algal mats at Sta. TL4. The cores were capped at both ends and injected at 1-cm intervals with carrier-free $^{35}SO_4$. The samples were then incubated under in situ conditions for 6–9 h, cut into 2 cm portions, then terminated by fixation in 20% zinc acetate. Time courses were run at Stas. TL5 and TB1 with incubations fixed hourly up to 12 h to ensure linear rates of radiolabel uptake. Samples were then frozen until a two-step distillation procedure (Fossing and Jorgensen 1989) was used to determine the fraction of reduced radiolabel shunted into the acid-volatile sulfide (AVS) and chromium-reducible (CRS) sulfur pools.

DIC and O_2 fluxes at the soil surface

Fluxes of DIC were measured in darkened chambers from inundated soils, and oxygen fluxes were measured in light and dark chambers from exposed and inundated soils, within each plot in 2008. Oxygen fluxes were also measured from exposed soils at Sta. TL4 in 2007.

For measurements from inundated soils, replicate ($n = 3$) opaque chambers (volume = 1 l; area = 82 cm^2) were gently placed into the soil and allowed to fill naturally with the incoming tide. Chambers were placed to avoid any obvious algal mats. Each chamber was closed at the top with a propeller-electric motor unit (Alongi et al. 2000). Samples for DIC were taken at 1 h intervals during 3–4 h incubation via a sampling port on the side of the chamber; the port was fitted with acid-washed Teflon tubing to draw off 2 ml samples. Replacement water was injected during sampling to avoid a vacuum. DIC was measured as described earlier. In these same chambers, dissolved O_2 was measured using a calibrated O_2 probe (TPS Model WP-82 DO meters) placed into a sampling port opposite the port for solute sampling. Prior to immersion by the incoming tide, these chambers were closed and used to measure O_2 concentrations over the exposed soil surface. O_2 readings were logged every 10 min for as long as the decline in O_2 concentrations was linear with time (usually 3 h). Rates of benthic gross primary production were estimated with the same techniques using triplicate clear chambers placed randomly within each plot. Rates of net primary production were determined by difference in O_2 flux rates between dark and light chambers and were calculated assuming 12 h daylight.

Statistics

Differences in some forest and soil parameters were tested using one- (site) or two-way (site × season) ANOVA (Sokal and Rohlf 1995) followed by Ryan's *Q*-test (Day and Quinn 1989) for multiple comparisons when significant main effects were found. In nearly all cases, data from replicate plots were pooled as preliminary analysis showed that differences among plots were not significant. If necessary, data are square-root transformed. Fluxes rates were determined by least-squares regression and relationships among variables (presented as r values) were explored using best-fit regression analysis. Results were compared at the 5% level of significance.

Results

Forest and soil characteristics

Station TB1 had significantly highest above-ground biomass (AGB), followed by Stas. TL5 > BC1 = TL6 > SL2 > TL4 = SL1 (Table 1). Station TB1 had the largest trees (mean DBH). Above-ground biomass correlated positively with canopy cover ($r = 0.85$) and LAI ($r = 0.77$). Canopy cover ($r = 0.92$), LAI ($r = 0.90$), and AGB ($r = 0.78$) across the seven forests correlated positively with salinity (Table 2) but negatively with topographic height (r range -0.77 to -0.90), as salinity declined with increasing tidal height ($r = -0.78$), excluding Sta. TL4 at the end of the dry season (Table 2).

Interstitial salinity, DIC, and solid-phase elements varied widely among forests and seasons (Table 2). Salinity ranged from 1 at Sta. SL1 to 55 at Sta. TL4, with higher salinities at the end of the dry season (October 2008) than at the end of the wet season (July 2007) at Stas.TL4 and TL5 (Table 2). Interstitial DIC concentrations were not significantly different from DIC concentrations in water from the drainage channels, but both were significantly greater than DIC in overlying tidal waters (Table 2). At Stas.TL4 and TL5, interstitial DIC values were greater at the end of the dry season (Table 2). Soil C:N (molar) ratios ranged from a low of 18 at Sta. BC1 to a high of 33 at Sta. TB1. Soil N:P ratios ranged from a low of 1.8 at Sta. TL1 to a high of 16.6 at Sta. TB1 and correlated positively with mangrove AGB ($r = 0.76$). Soil nitrogen ($r = 0.90$) and total organic carbon ($r = 0.83$) also correlated positively with above-ground biomass.

O_2 and DIC fluxes at the soil surface

Differences in respiration rates under both exposed and inundated conditions (Table 3) were inconsistent. At Stas.TL4, BC1, TL6 and TB1, the differences between tidal conditions were not significant; at Sta. TL5, O_2 consumption rates were significantly greater from inundated soils, whereas at Stas. SL1 and SL2, respiration rates were greater from exposed soils. Differences between rates measured in 2007 and 2008 at Sta. TL4 were not significant. Respiration rates related positively to topographical height ($r = 0.80$) but negatively with above-ground biomass

Table 1 Stand characteristics of the seven mangrove forests sampled in Timor Leste

Characteristics	Forest sites						
	TL4	TL5	BC1	SL1	SL2	TL6	TB1
AGB[a]	136.1 ± 14.6	375.2 ± 12.5	315.4 ± 12.3	108.8 ± 16.1	171.6 ± 15.3	300.0 ± 18.7	492.9 ± 16.7
Mean dbh[b]	6.1 ± 1.3	7.1 ± 1.3	7.5 ± 1.1	12.2 ± 0.1	11.2 ± 0.7	24.1 ± 2.9	44.7 ± 1.1
Forest canopy cover (η)	0.72 ± 0.06	0.91 ± 0.07	0.85 ± 0.09	0.52 ± 0.08	0.63 ± 0.04	0.90 ± 0.09	0.89 ± 0.06
LAI[c]	2.2 ± 0.1	4.4 ± 0.2	4.1 ± 1.0	1.4 ± 0.1	2.5 ± 0.1	5.4 ± 0.4	4.1 ± 0.03
Topographic height[d]	100	10	150	250	220	40	20
Stem density[e]	11,447 ± 595	11,217 ± 627	20,410 ± 834	3,316 ± 169	7,985 ± 222	15,269 ± 593	7,448 ± 216
Basal area[f]	11 ± 1	17.0 ± 2	46 ± 2	16 ± 3	18 ± 2	27 ± 2	32 ± 5

Values are mean ± 1 SE from triplicate plots within each forest

[a] Total above-ground biomass (t DW ha^{-1})

[b] Diameter-at-breast height (cm)

[c] Leaf area index (m^2 leaf area m^{-2} ground area)

[d] cm above mean sea-level

[e] No. stem ha^{-1}

[f] m^2 ha^{-1}

Table 2 Salinity, particulate nutrient, and DIC concentrations from soils taken to 50 cm depth from replicate wells at the seven mangrove forests

	TL4	TL5	BC1	SL1	SL2	TL6	TB1
OW salinity	8[a], 12[b]	20[a], 22[b]	44	5	25	35	35
PW salinity	21[a], 55[b]	27[a], 28[b]	31	1	20	38	36
PW-DIC[c]	13.6 ± 0.1[a] 54.8 ± 1.2[b]	14.3 ± 0.4[a] 34.7 ± 1.3[b]	23.4 ± 0.1	11.4 ± 0.2	13.2 ± 0.2	17.5 ± 0.3	9.5 ± 0.2
OW-DIC[c]	4.8 ± 0.5[a] 8.1 ± 0.1[b]	4.7 ± 0.2[a] 6.7 ± 0.1[b]	5.8 ± 0.4	3.3 ± 1.2	4.0 ± 0.8	3.6 ± 0.4	3.8 ± 0.5
Drainage DIC[c]	14.0 ± 1.6[a] 55.2 ± 0.9[b]	14.4 ± 0.4[a] 35.5 ± 1.2[b]	30.0 ± 4.6	13.9 ± 1.6	14.6 ± 2.0	17.1 ± 0.4	8.7 ± 1.0
TOC[d]	0.81 ± 0.10	3.31 ± 0.13	1.98 ± 0.33	1.46 ± 0.24	2.79 ± 0.39	3.80 ± 0.19	9.82 ± 0.15
TN[e]	0.05 ± 0.01	0.19 ± 0.01	0.13 ± 0.01	0.08 ± 0.01	0.14 ± 0.01	0.16 ± 0.01	0.35 ± 0.01
TP[f]	607 ± 111	656 ± 10	498 ± 7	542 ± 21	580 ± 12	539 ± 14	452 ± 7

Values are mean ± 1 SE from triplicate samples taken from each well within each forest

[a] July 2007 (end of wet season)

[b] October 2008 (end of dry season)

[c] Dissolved inorganic carbon, mmol l^{-1}

[d] Total soil organic carbon (% soil DW)

[e] Total soil nitrogen (% soil DW)

[f] Total soil phosphorus (ppm)

PW porewater, *OW* overlying tidal water

Table 3 Rates of bacterial sulfate reduction (SRR, mmol S m^{-2} d^{-1}), benthic microalgal net primary production (NPP, mmol O_2 m^{-2} d^{-1}) and O_2 (DRO) and DIC (DRC) respiration (mmol m^{-2} d^{-1}) from exposed and inundated soils at the seven mangrove forests in Timor Leste

Location, date and soil condition	DRO	NPP	DRC	SRR
TL 4				
2007 (exposed)	69.8 ± 12.6	NA		1.9 ± 0.1 (0–40)
2007 (algal mat)				16.3 ± 3.8 (0–10)
2008 (exposed)	59.3 ± 13.3	18.3 ± 12.0		2.1 ± 0.2 (40–50)[a]
2008 (inundated)	47.2 ± 6.9	11.0 ± 7.4	67.4 ± 7.1	49.6 ± 4.4 (0–40)
TL 5				
2007 (exposed)				24.0 ± 6.6 (0–80)
2008 (exposed)	15.7 ± 5.6	0.05 ± 0.6		31.4 ± 0.6 (0–80)
2008 (inundated)	69.1 ± 7.1	16.8 ± 12.3	81.2 ± 13.4	34.4 ± 9.1 (0–80)
BC 1				
2008 (exposed)	27.9 ± 6.6	NA		53.9 ± 13.3 (0–80)
2008 (inundated)	37.3 ± 6.4	NA	60.5 ± 9.5	57.3 ± 9.4 (0–80)
SL1				
2008 (exposed)	123.9 ± 36.8	32.5 ± 8.6		112.2 ± 28.9 (0–40)
2008 (inundated)	67.3 ± 18.6	9.8 ± 6.7	100.0 ± 11.2	NA
SL2				
2008 (exposed)	98.4 ± 4.0	30.6 ± 2.6		101.8 ± 53.6 (80)
2008 (inundated)	67.5 ± 9.9	19.9 ± 6.6	102.5 ± 8.8	NA
TL6				
2008 (exposed)	52.7 ± 9.3	2.1 ± 5.9		58.4 ± 10.9 (80)
2008 (inundated)	48.7 ± 9.3	15.7 ± 4.4	118.2 ± 5.2	60.3 ± 18.8 (70)
TB1				
2008 (exposed)	18.5 ± 9.9	0.7 ± 0.4		115.2 ± 48.0 (20)
2008 (inundated)	15.2 ± 2.8	4.3 ± 2.8	223.5 ± 7.6	108.3 ± 22.2 (20)

Values are mean ± 1 SE of triplicate cores per plot in each forest. Values in parentheses are maximum depths of core penetration

[a] Too dry to sample from surface to 40 cm depth

($r = -0.90$), LAI ($r = -0.74$), and salinity ($r = -0.85$).

Rates of benthic NPP (Table 3) were also inconsistent among sites between exposed and inundated conditions. NPP rates were not significantly different between tidal conditions at Sta. TL4, but were significantly greater on exposed soils at Stas. SL1 and SL2 and were significantly greater on inundated soils at Stas.TL5, TL6, and TB1. Rates of NPP on exposed soils correlated negatively with increasing mangrove canopy cover (Fig. 2, top graph), but not when inundated (Fig. 2, bottom graph). NPP also correlated significantly with respiration, with a positive linear relationship under both exposed and inundated conditions (Fig. 3).

Rates of dark DIC release from inundated soils (Table 3) varied among sites as follows:

TB1 > TL6 > SL2 = SL1 = TL5 > TL4 = BC1. DIC release rates did not correlate with rates of dark O_2 respiration or NPP, but did relate positively with soil TOC ($r = 0.95$), soil TN ($r = 0.87$) and soil C:N ($r = 0.95$) and N:P ($r = 0.93$). The ratio of DIC:O_2

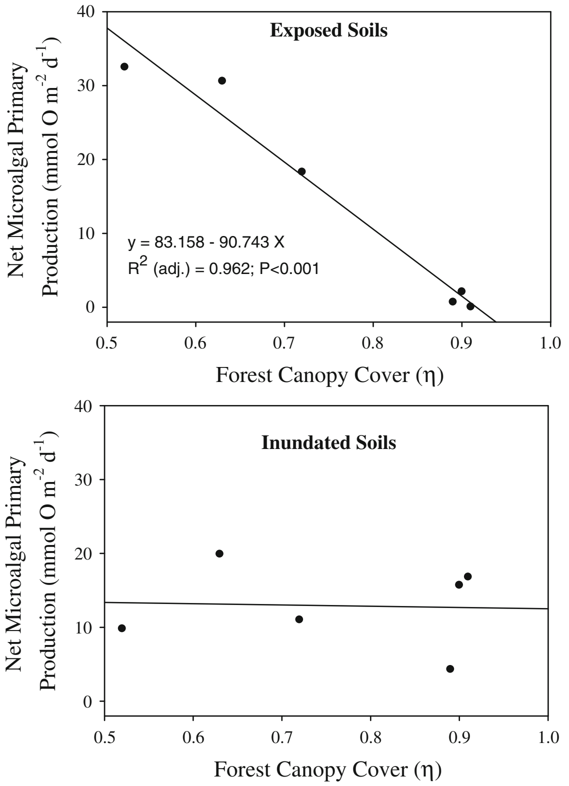

Fig. 2 Linear relationship between forest canopy cover and benthic net primary production in (*top graph*) air-exposed chambers and (*bottom graph*) the lack of a relationship under inundated conditions, across all seven forests

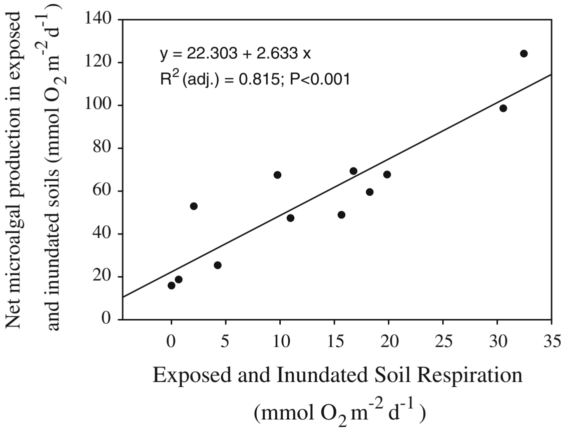

Fig. 3 Linear relationship between benthic net primary production and soil respiration in both air-exposed and tidally inundated chambers. The data encompass oxygen measurements taken at all seven forests

flux from inundated soils ranged from 1.2 to 1.6 among sites TL4, TL5, BC1, SL1 and SL2, 2.4 at Sta. TL6 and 14.7 at Sta. TB1.

Sulfate reduction

Rates of sulfate reduction (SRR) varied significantly with soil depth and location (Table 3), with increasing rates with greater depth at Stas.TL4 (2007, 2008), SL1, SL2, and TL6 and with no clear depth-related patterns at Stas.TL5 (2007, 2008), BC1, and TB1 (depth data not shown). Volume-specific rates of sulfate reduction at Sta. TL4 in 2007 were significantly greater within a surface algal mat than in soils devoid of surface mats (Table 3). Soils were too dry in 2008 to sample over the upper 40 cm, but wet enough to sample at the 40–50 cm horizon. Once inundated, 0–40 cm samples were taken at Sta. TL4 and showed active SRR (Table 3). Differences between years and between exposed and inundated conditions at Sta. TL5 were not significant. The lack of change due to tidal conditions was true for the other sites. Under exposed conditions in 2008, volume-specific rates of sulfate reduction at Sta. TL5 were significantly lower than at the other sites (excluding Sta. TL4) which had equivalent rates. SRR did not relate to rates of O_2 or DIC flux. The only significant correlations were positive exponential relationships of SRR with soil TOC and TN concentrations across sites and soil depths (Fig. 4).

Discussion

A fundamental assumption of using measurements of rates of CO_2 release or O_2 consumption across the soil–water/air interface as an estimate of total community metabolism is that steady-state conditions exist. That is, conditions remain constant such that fluxes across the soil–water interface are equal to depth-integrated remineralization rates (Burdige 2006). Evidence increasingly suggests that steady-state conditions in intertidal environments are not as common as previously believed (Burdige 2006). The sediment deposits of many tidal flats and wetlands thus act as a filter through which porewater is pumped advectively by tides (Rusch and Huettel 2000; Huettel and Webster 2001).

The forest floor of most mangroves consists of soils of varying porosity, interspersed with numerous cracks, fissures, holes, and invertebrate tubes and burrows, through which salts and solutes are transported during tidal infilling and draining (Mazda and

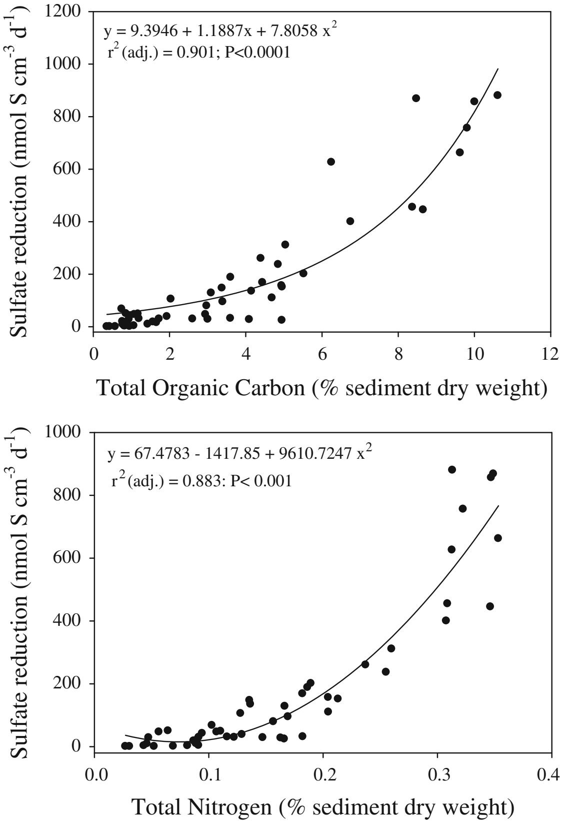

Fig. 4 Exponential relationship of sulfate reduction with (*top graph*) soil total organic carbon and (*bottom graph*) total nitrogen, at soil intervals where both parameters were measured within all seven forests

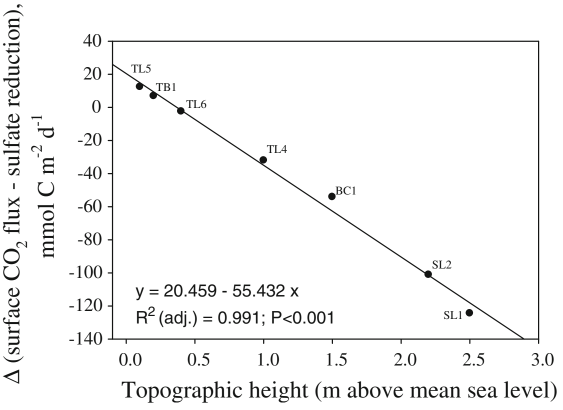

Fig. 5 Plot showing increasing differences between rates of microbial metabolism in surface soils and carbon mineralized via sulfate reduction, with increasing topographic height. Differences tabulated from season-averaged data in Table 3

Ikeda 2006). Seepage of groundwater through the forest floor is controlled by a number of physical forces (Mazda et al. 1990; Susilo et al. 2005; Mazda and Ikeda 2006) that result in interstitial water oozing out through the bottom soil, most clearly seen as water moving through seepage channels between the forest and adjacent creek bank. In this study, we sampled water in drainage channels from all seven sites and found that DIC concentrations in the seepage were equivalent to those measured in the interstitial water (with both greater than overlying DIC water concentrations) showing that mineralized carbon is being drained advectively from these forests.

We suggest that tidal advection is occurring in these Timorese mangroves, resulting in subsurface transport of mineralized carbon from the forest that is not accounted for in the flux measurements across the soil surface. Four pieces of evidence support this notion: (1) DIC concentrations in drainage water were equivalent to those in the porewater; (2) rates of DIC and O_2 flux did not correlate with rates of sulfate reduction; (3) rates of volume-specific sulfate reduction, converted to carbon assuming a 2:1 molar ratio of C:S (Burdige 2006), were much greater than flux rates at the soil surface; and (4) the discrepancy between the rates of sulfate reduction and surface mineralization increased with increasing topographic height (Fig. 5). These discrepancies may be even greater considering that other microbial processes such as iron and manganese reduction were probably active in subsurface soils, especially as oxygen and other gases probably penetrate deeper into the forest floor when exposed. CO_2 release in air-exposed chambers was not measured but such rates would likely be greater than DIC fluxes.

Our data suggests that surface metabolism may be uncoupled from subsurface metabolism, with O_2 and DIC fluxes at the soil surface more closely reflecting intense microalgae-bacteria interrelationships, than efflux of reduced metabolites from deeper, subsurface deposits. This is reflected in the correlations of benthic NPP with available light and with oxygen consumption. Rates of volume-specific sulfate reduction related most closely to TOC and TN concentrations in subsurface soils rather than to any processes measured at the soil surface. Correlation is not causation, but these correlations are in agreement with earlier mangrove studies which observed significant relationships between sulfate reduction and biomass of live fine roots (Alongi 2005). Obviously, other factors also regulate metabolic processes, such as temperature, extent of burrowing crab activities, and rates of organic matter supply.

This interpretation, if accurate, would help to explain similar discrepancies between rates of subsurface anaerobic metabolism and surface measurements of CO_2 and O_2 flux found in other forests (Kristensen et al. 1988, 2008; Nedwell et al. 1994; Alongi 2001). In Jamaican mangroves, for example, discrepancies between these processes were attributed to subsurface reoxidation and to release of DOC from roots stimulating sulfate reduction (Nedwell et al. 1994), but we note that the largest discrepancies were at the high forest site. Comparisons with mangrove studies other that those cited above are problematic, because sulfate reduction was underestimated in earlier studies being measured only in the upper few cm. It is now known that active reduction can occur to depths of at least 1 m (Alongi 2005), so it is likely that similar discrepancies exist in other forests. Similar arguments have been offered to explain discrepancies between surface and subsurface metabolism with increasing tidal elevation from low to high marshes (Howes and Goehringer 1994; Gribsholt and Kristensen 2003). Subterranean loss of solutes is significant in some intertidal habitats, but not in others, with bed slope, soil texture, elevation above mean sea-level, and tidal range, being some of the major determinants of the extent of groundwater discharge.

Our finding that significant amounts of mineralized carbon are lost via subsurface flow supports the recent studies of DIC flow from mangrove creek waters (Bouillon et al. 2007; Biswas et al. 2004; Koné and Borges 2008; Miyajima et al. 2009) as well as carbon flow models for mangrove forests (Bouillon et al. 2008a; Alongi 2009). The waterway studies consistently found that mangrove waters are oversaturated in CO_2 as a direct result of pelagic respiration and porewater DIC being transported laterally by tidal pumping to the adjacent tidal creeks. Evidence for the latter pathway was gleaned from the fact that creek DIC concentrations varied in synchrony with the tide; creeks at low tide consistently contain significantly greater DIC concentrations than creeks at high tide.

The importance of inorganic carbon flow in mangrove creeks and waterways as established by these studies is reflected in the most recent budgets of mangrove carbon cycling (Bouillon et al. 2008a; Alongi 2009). The budget of Bouillon et al. (2008a) found that >50% of carbon fixed by mangroves, roughly112 Tg C year^{-1}, is unaccounted for by known pathways. Alongi (2009) calculated a similar figure (160 Tg C year^{-1}), and both global budgets suggest that the 'missing' carbon is respired DIC being advected from and transported from tidal creeks to adjacent coastal waters. These budgets and the data presented here are indicative, not absolute, but they do point to a pathway of C loss from mangroves that must be considered in future. Considering that mangroves allocate a large proportion of their fixed carbon belowground (Lovelock 2008), metabolic rates within the mangrove forest floor and adjacent waterways have been seriously underestimated, and may well be the principal pathway by which inorganic carbon is lost from these systems to the adjacent coastal ocean.

Other factors help to regulate soil metabolic processes. For instance, the decline in tree size with increasing tidal height results in more canopy gaps and thus more light penetrating to the forest floor. Less canopy cover (more light) results in greater rates of net primary production on the soil surface during air exposure, which in turn stimulates oxygen consumption at the soil-air interface (Fig. 3). Control by available light is further illustrated by the difference in rates of net primary production in air-exposed versus inundated chambers (Fig. 2). The simplest explanation is that when the chambers are flooded with silt-laden tidal water, available light levels drop below a threshold sufficient to stimulate rates of microalgal primary production above $\approx$20 mmol O_2 m^{-2} d^{-1}. However, the slope of the regression relationship between NPP and soil respiration (Fig. 3) indicates that microalgal NPP is nearly three times greater than surface soil respiration. Our data confirm earlier observations of lower NPP on soils beneath mangrove canopies compared with rates measured on adjacent sand and mudflats (Kristensen et al. 1988; Alongi 1994). The rates of benthic primary production measured in Timor Leste are at the low end of the range of rates measured on tidal flats (Colijn and de Jonge 1984) but are mid-range compared with rates measured in other mangrove forests (Kristensen et al. 1988; Alongi 1994).

Rates of benthic primary production are dwarfed by rates of forest net primary production. Crude estimates of forest NPP (NPP = A × LAI × daylight hours) using the LAI values (Table 1) and an average rate of leaf photosynthesis (A) of 12 μmol CO_2 m^{-2} s^{-1} (Alongi 2009) indicate a range of forest NPP from 725 to 2800 mmol C m^{-2} d^{-1}, well within the range of rates for dry tropical mangroves (Alongi et al. 2000) and at least an order of magnitude greater than rates of benthic NPP in these forests (Table 3).

Rates of DIC release from inundated soils did not correlate with either benthic primary production or oxygen consumption, but did correlate with soil carbon and nitrogen content. O_2 consumption in dark chambers represents aerobic respiration as well as oxidation of reduced metabolites diffusing across the soil–water interface and may not be directly equivalent to rates of DIC release, especially when algal mats and carbonate are present, or under non-steady state conditions. The ratio of DIC:O_2 flux in low carbonate and carbonate-free mangrove soils averages 1.6 and 1.3 under inundated and air-exposed conditions, respectively (Alongi 2009). However, we measured ratios of 2.4 at site TL6, 14.7 at site TB1 and a narrow range of ratios (1.2–1.6) among the other five forests. The results from the former two sites are discordant; the high ratio at site TB1 may reflect comparatively greater contribution of DIC release from tree roots than at the other sites because we observed that the bulk of the roots of these very large trees were restricted to the very shallow (20 cm) unconsolidated soil column.

The source of the organic matter being mineralized also plays an important role in rates and pathways of bacterial mineralization. We observed significant positive correlations of DIC release and the ratio of DIC:O_2 respiration with soil C:N and N:P ratios. The highest stoichiometric ratios were measured at sites TB1 and TB6, where large pools of mangrove litter were observed lying on the forest floor. These detritus pools appeared and smelled sulfidic; the presence of these detritus patches suggests that oxidation of sulfides was incomplete. The presence of algal mats in the other forests with more open canopies may foster more closely linked aerobic and anaerobic carbon oxidation at the soil surface. At these sites, the DIC:O_2 ratios were within those expected for the complete oxidation of model Redfield ratio organic matter (1.3) and of average marine microalgae or plankton (1.45), suggesting that most organic matter decomposing at the soil surface was of algal, and not vascular plant, origin.

Acknowledgments Bob Wasson is thanked for the pleasure of his company and help during the field trips, as are many members of MAFF for logistics and field help. S. Boyle, C. Payn, J. Wu Won, and F. Patel performed some of the chemical analyses. Two anonymous reviewers are thanked for helpful comments. This study was funded by the Democratic Republic of Timor Leste and the Australian Institute of Marine Science.

References

Alongi DM (1994) Zonation and seasonality of benthic primary production and community respiration in tropical mangrove forests. Oecologia 98:320–327

Alongi DM (2001) The influence of mangrove biomass and production on biogeochemical processes in tropical macrotidal coastal settings. In: Aller JY, Woodin SA, Aller RC (eds) Organism–sediment interactions. University of South Carolina Press, Columbia

Alongi DM (2005) Mangrove-microbe-soil relations. In: Kristensen E, Haese RR, Kostka JE (eds) Interactions between macro- and microorganisms in marine sediments. American Geophysical Union, Washington

Alongi DM (2009) The energetics of mangrove forests. Springer, Dordrecht

Alongi DM, Tirendi F, Clough BF (2000) Below-ground decomposition of organic matter in forests of the mangroves *Rhizophora stylosa* and *Avicennia marina* along the arid coast of western Australia. Aq Bot 68:97–122

Alongi DM, Wattayakorn G, Pfitzner J et al (2001) Organic carbon accumulation and metabolic pathways in soils of mangrove forests in southern Thailand. Mar Geol 179:85–103

Biswas H, Mukhopadhyay SK, De TK, Sen S, Jana TK (2004) Biogenic controls on the air–water carbon dioxide exchange in the Sunderbans mangrove environment, northeast coast of Bay of Bengal, India. Limnol Oceanogr 49:95–202

Bouillon S, Middelburg JJ, Dehairs F et al (2007) Importance of intertidal soil processes and porewater exchange on the water column biogeochemistry in a pristine mangrove creek (Ras Dege, Tanzania). Biogeosciences 4:311–322

Bouillon S, Borges A, Castaneda-Moya E et al (2008a) Mangrove production and carbon sinks: a revision of global budget estimates. Global Biogeochem Cycles 22:GB2013. doi:10.1029/2007GB003OS2

Bouillon S, Connolly RM, Lee SY (2008b) Organic matter exchange in mangrove ecosystems: recent insights from stable isotope studies. J Sea Res 59:44–58

Burdige DJ (2006) Geochemistry of marine sediments. Princeton University Press, Princeton

Cintron G, Novelli YS (1984) Methods for studying mangrove structure. In: Snedaker SC, Snedaker JG (eds) The mangrove ecosystem: research methods. UNESCO, Paris

Clough BF (1997) Mangrove ecosystems. In: English S, Wilkinson C, Baker V (eds) Survey manual for tropical marine resources, 2nd edn. Australian Inst Mar Sci, Townsville

Colijn F, de Jonge VN (1984) Primary production of microphytobenthos in the Ems-Dollard estuary. Mar Ecol Prog Ser 14:185–196

Day RW, Quinn GP (1989) Comparisons of treatments after an analysis of variance in ecology. Ecol Monogr 59:433–463

Durand E (2002) East Timor: a country at the crossroads of Asia and the Pacific. Silkworm Books, Chiang Mai

Fossing HR, Jorgensen BB (1989) Measurement of bacterial sulfate reduction in soils: evaluation of a single-step chromium reduction method. Biogeochem 8:205–222

Gribsholt B, Kristensen E (2003) Benthic metabolism and sulfur cycling along an inundation gradient in a tidal *Spartina anglica* salt marsh. Limnol Oceanogr 48:2151–2162

Hall POJ, Aller RC (1992) Rapid, small-volume flow injection analysis for $\sum CO_2$ and NH_4^+ in marine and freshwaters. Limnol Oceanogr 37:1113–1118

Heron SF, Ridd PV (2008) The tidal flushing of multiple-loop animal burrows. Estuar Coastal Shelf Sci 78:135–144

Howes BL, Goehringer DD (1994) Porewater drainage and dissolved organic carbon and nutrient losses through the intertidal creekbanks of a New England salt marsh. Mar Ecol Prog Ser 114:289–301

Huettel M, Webster IT (2001) Porewater flow in permeable soils. In: Boudreau BP, Jørgensen BB (eds) The benthic boundary layer. Oxford University Press, Oxford

Komiyama A, Poungparn S, Kato S (2005) Common allometric equations for estimating the tree weight of mangroves. J Trop Ecol 21:471–477

Koné YJ-M, Borges AV (2008) Dissolved inorganic carbon dynamics in the waters surrounding forested mangroves of the Ca Mau province (Vietnam). Estuar Coast Shelf Sci 77:409–421

Kristensen E (2007) Carbon balance in mangrove soils: the driving processes and their controls. In: Tateda Y et al (eds) Greenhouse gas and carbon balances in mangrove coastal ecosystems. Gendai Tosho, Japan

Kristensen E (2008) Mangrove crabs as ecosystem engineers; with emphasis on soil processes. J Sea Res 59:30–43

Kristensen E, Alongi DM (2006) Control of fiddler crabs (*Uca vocans*) and plant roots (*Avicennia marina*) on carbon, iron, and sulphur biogeochemistry in mangrove soil. Limnol Oceanogr 51:1557–1571

Kristensen E, Andersen FØ, Kofoed LH (1988) Preliminary assessment of benthic community metabolism in a south-east Asian mangrove swamp. Mar Ecol Prog Ser 48:137–145

Kristensen E, Bouillon S, Dittmar T, Marchand C (2008) Organic carbon dynamics in mangrove ecosystems: a review. Aq Bot 89:201–219

Loring DH, Rantala RTT (1992) Manual for the geochemical analysis of marine sediments and suspended particulate matter. Earth Sci Rev 32:235–283

Lovelock CE (2008) Soil respiration and belowground carbon allocation in mangrove forests. Ecosystems 11:342–354

Lustwerk RL, Burdige DJ (1995) Elimination of dissolved sulfide interference in the flow injection determination of ΣCO_2 by addition of molydate. Limnol Oceanogr 40:1011–1012

Mazda Y, Ikeda Y (2006) Behavior of the groundwater in a riverine-type mangrove forest. Wetlands Ecol Manag 14:477–488

Mazda Y, Yokochi H, Sato Y (1990) Groundwater flow in the Bashita-minato mangrove area, and its influence on water and bottom mud properties. Estuar Coast Shelf Sci 31:621–638

Miyajima T, Tsuboi Y, Tanaka Y et al (2009) Export of inorganic carbon from two southeast Asian mangrove forests to adjacent estuaries as estimated by the stable isotope composition of dissolved inorganic carbon. J Geophys Res 114:G01024. doi:10.1029/2008JG000861

Nedwell DB, Blackburn TH, Wiebe WJ (1994) Dynamic nature of the turnover of organic carbon, nitrogen and sulphur in the soils of a Jamaican mangrove forest. Mar Ecol Prog Ser 110:223–231

Ridd PV (1996) Flow through animal burrows in mangrove creeks. Estuar Coast Shelf Sci 43:617–625

Rusch A, Huettel M (2000) Advective particle transport into permeable soils—evidence from experiments in an intertidal sandflat. Limnol Oceanogr 45:525–533

Saenger P (2002) Mangrove ecology. Silviculture and Conservation, Kluwer

Sokal RR, Rohlf FJ (1995) Biometry, 3rd edn. WH Freeman, San Francisco

Susilo A, Ridd PV, Thomas S (2005) Comparison between tidally driven groundwater flow and flushing of animal burrows in tropical mangrove swamp. Wetlands Ecol Manag 13:377–388